SESAME

Synchrotron-light For Experimental Science and Applications In The Middle East

IBIC 2026

Diagnostics devices, challenges and developments at the SESAME light source

Hussein Al-Mohammad

On behalf of SESAME Staff

IBIC 2026, Whistler, BC, Canada

SESAME

Outline

- **Introduction to SESAME**
- **Facility Status**
- **Beam position stability**

  (TUP043) Beam position stability and global orbit feedback system at SESAME
- **Beam size measurement**

  (MOP049) Development of In-Air X-ray Detector for vertical beam size measurement at SESAME
- **Injection efficiency**

  (TUP044) Injection efficiency measurement at SESAME
- **Conclusion**

Introduction to SESAME

First 3rd Generation Synchrotron Light Source in Middle East, located in Allan, Jordan

SESAME Members
Associate members : Germany and Italy

SESAME

A light Converter

- A new term comes to life since 2019….. We Convert Sun Light to X-Rays ! 1st synchrotron light source fully powered by solar energy
- 6.5 MW Solar power plant.
- Achieved around $22 million in energy cost savings since commissioning
- Reduced CO_2 emissions by ~ 25,000 metric tons up to date

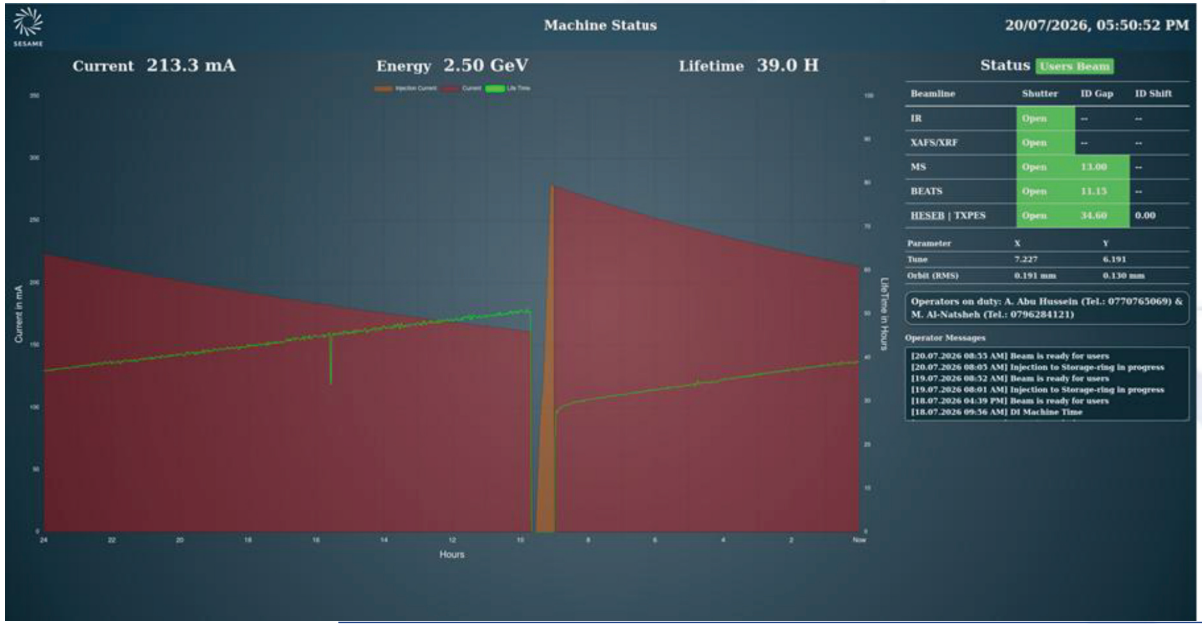

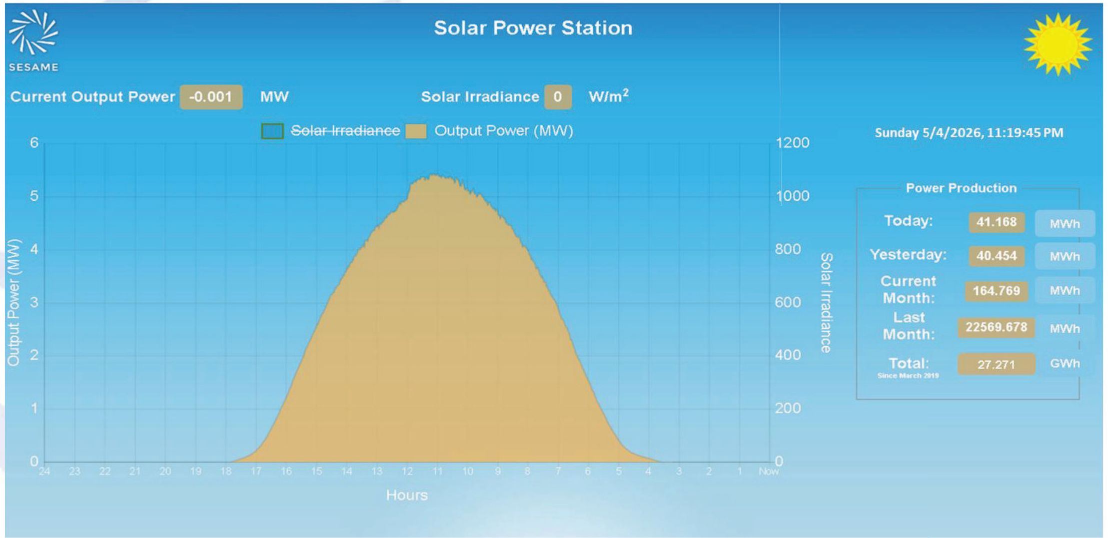

SESAME Structure

2.5GeV Storge Ring

- C =133.2m
- ε_x = 26 nm.rad
- Simple DBA lattice, dispersive sections
- 16 cells & 16 S.S. (8x4.2m + 8x2.2m)
- I = 300mA (design value: 400mA)
- RF: 500MHz, 1.7MV

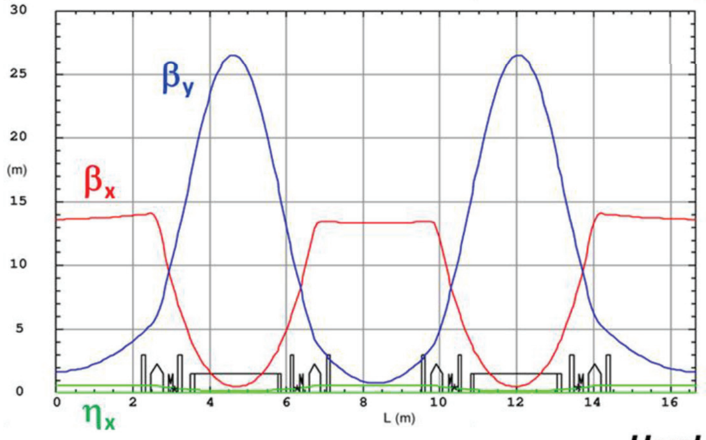

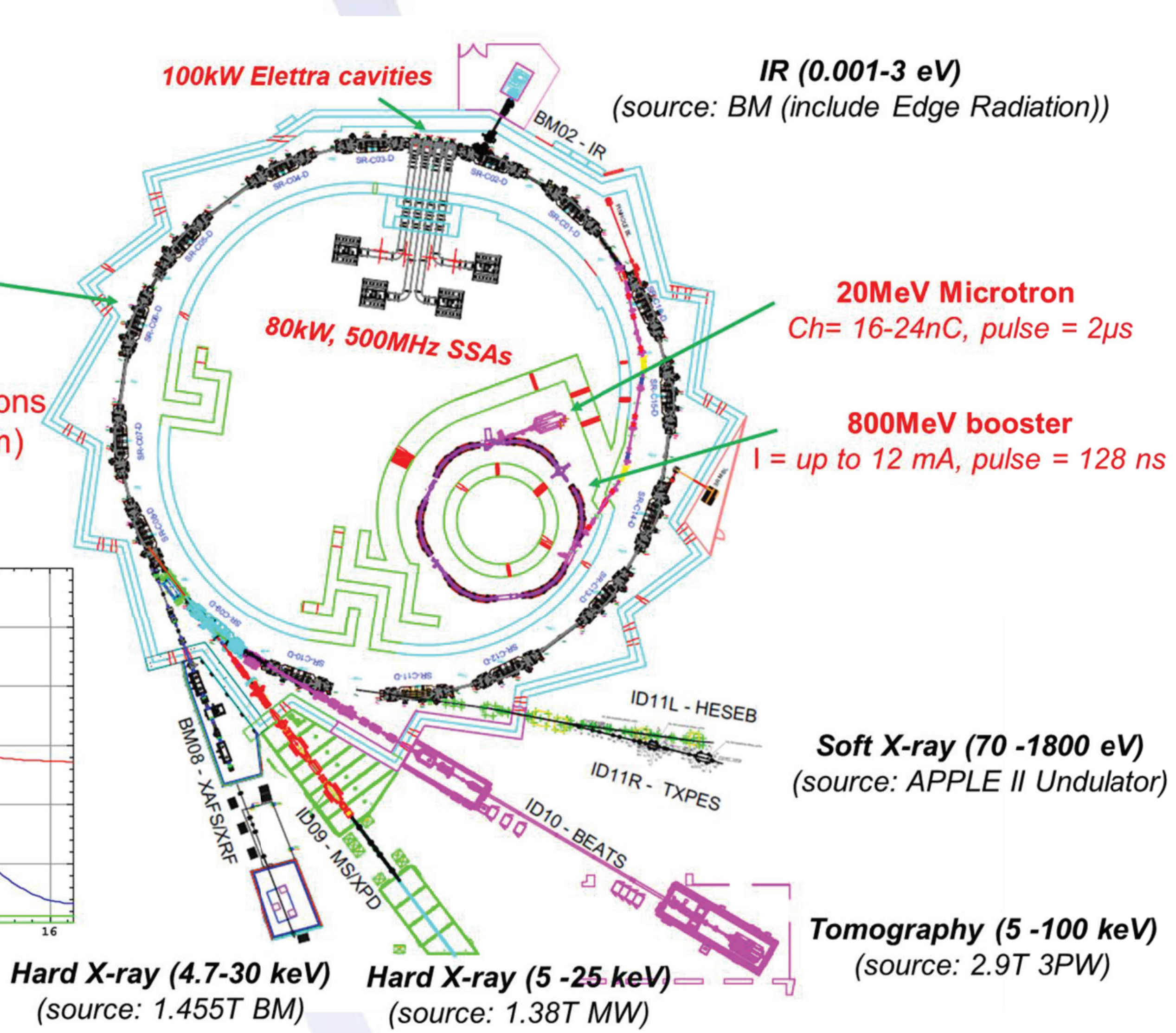

Beam Position Stability

Beam Position

- The SESAME SR is equipped with 64 physical BPMs, of which 48 are currently connected to Libera Brilliance+ electronics. Each Libera chassis can accommodate up to four BPM modules,
- 12 Libera units are installed , 10 of them hosts Gigabit Data Exchange (GDX) modules.
- Well calibrated coaxial cables with low attenuation LMR-240-FR with phase matching .
- Good beam position performance with low drift ~ 1µm over ~16 hours of beam decay.

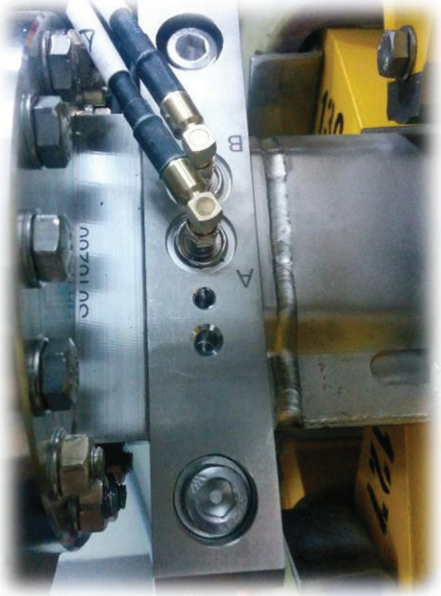

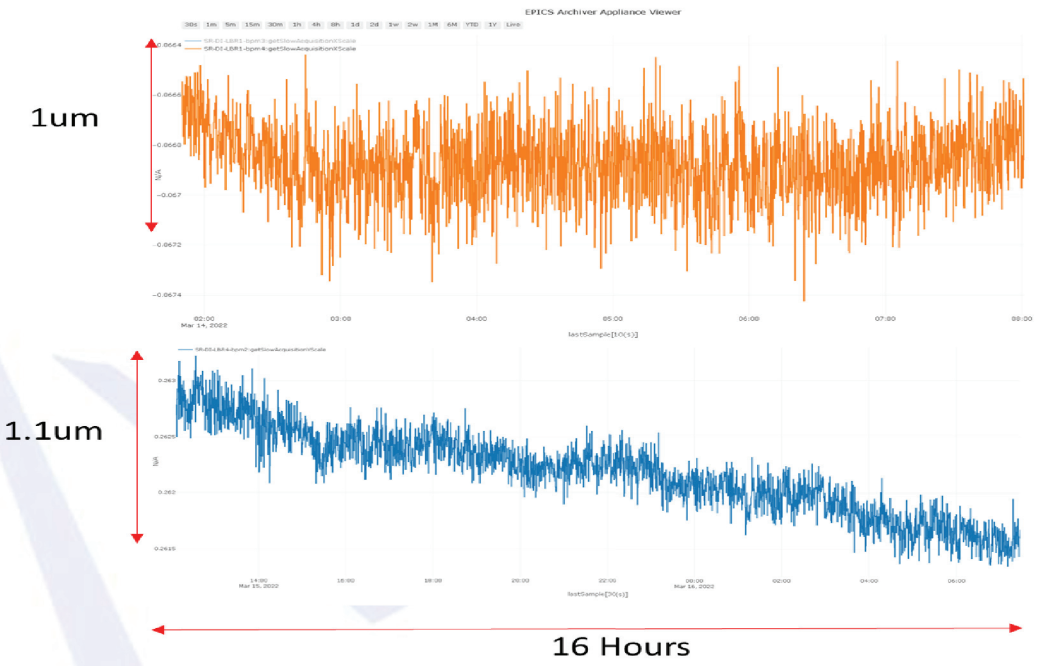

Beam Position Stability-SOFB

TUP043

- Since becoming a user facility in 2017, SESAME has employed a Slow Orbit Feedback (SOFB) system, implemented in MATLAB, to stabilize the global orbit of the Storage Ring (SR) at a low correction rate of 0.2 Hz sampling rate
- However, achieving improved synchrotron performance requires sub-micron beam orbit stability across a broader frequency range, extending up to 100 Hz. To address this, the SOFB system has been upgraded to operate at 10 Hz sampling rate using an in-house developed control system written in C, marking an important first step toward a Fast Orbit Feedback (FOFB) system.

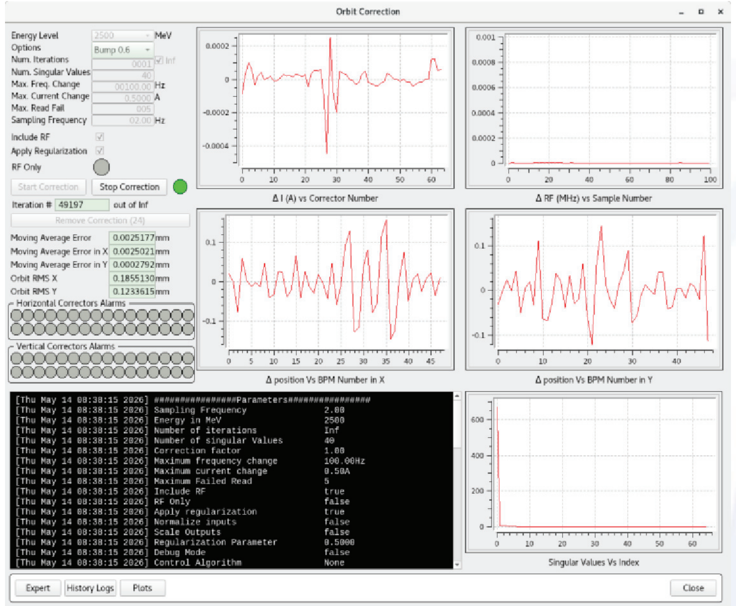

A. Aljadaa et al., “Towards fast orbit correction: a modular and extensible global orbit feedback system”, in Proc. IPAC’26, doi:10.18429/JACoW-IPAC2026-WEP6114

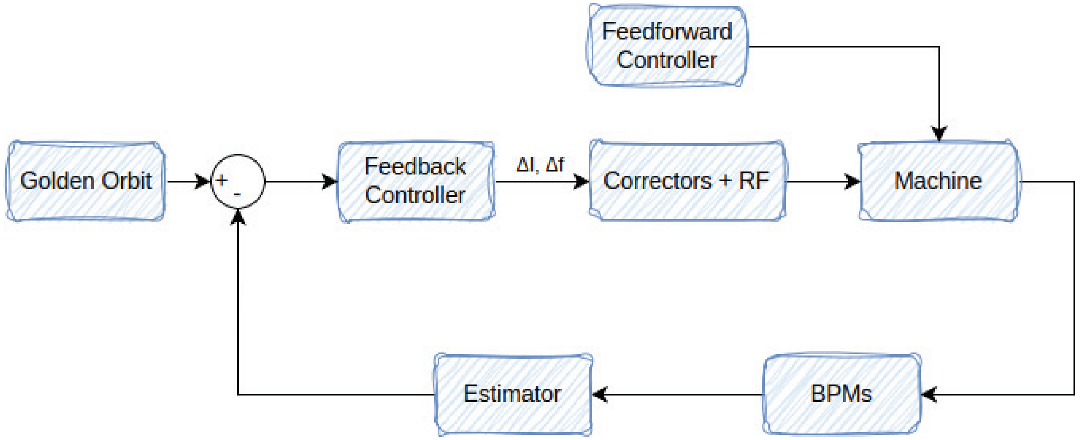

Orbit correction system architecture

Beam Position Stability-SOFB

The performance of the upgraded SOFB was evaluated during routine user operation by analyzing the beam position evolution over representative SR fills. Orbit deviations were calculated relative to the operational golden orbit using the 48 BPMs included in the feedback. The global horizontal and vertical RMS orbit errors were then evaluated as a function of time in order to characterize both short-term stability and long-term drift

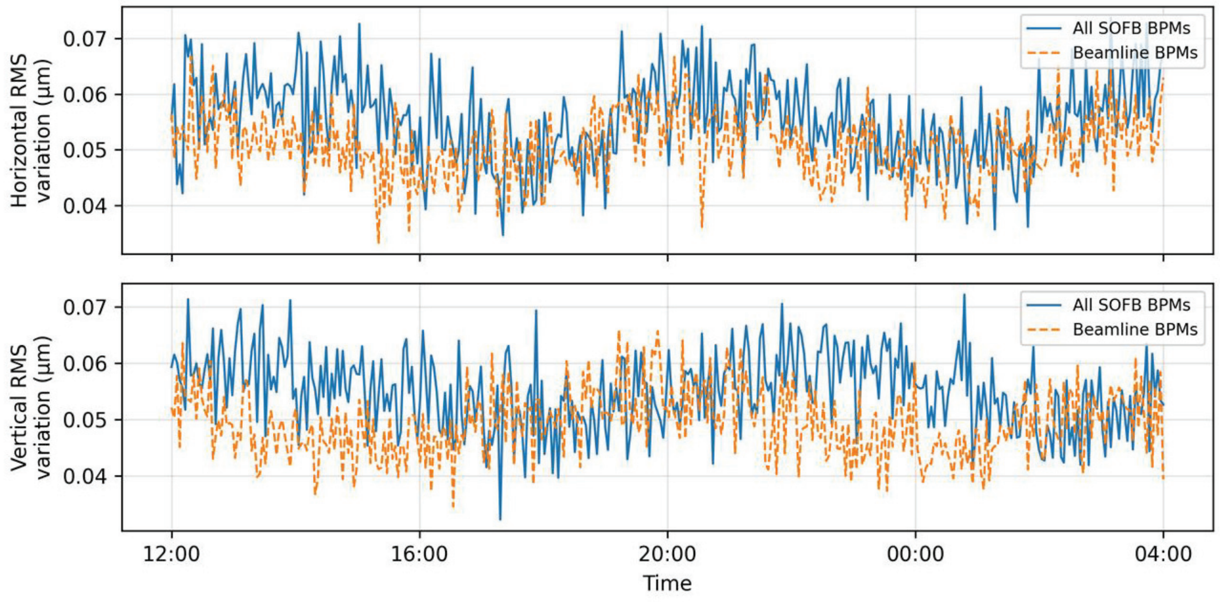

Sub-µm

short-term RMS variation

< 10%

beam-size stability target

48 BPMs

global evaluation

Result: orbit motion remained comfortably within the adopted beam-stability criterion during routine user operation.

Short-term horizontal and vertical RMS orbit variation during user operation period. The solid curves show the RMS variation calculated from all SOFB BPMs, while the dashed curves show the corresponding values for the BPMs adjacent to the operating beamlines.

Beam Position Stability-SOFB

Variation of Insertion Device (ID) parameters during user operation introduces reproducible perturbations to the electron orbit. To reduce these disturbances before they are handled by global orbit feedback, Feed-Forward compensation is applied during insertion device motion. The compensation is based on correction tables obtained from measured orbit responses as a function of the ID operating parameters. Feedforward suppresses the predictable part of the orbit perturbation, while the SOFB corrects the remaining residual error.

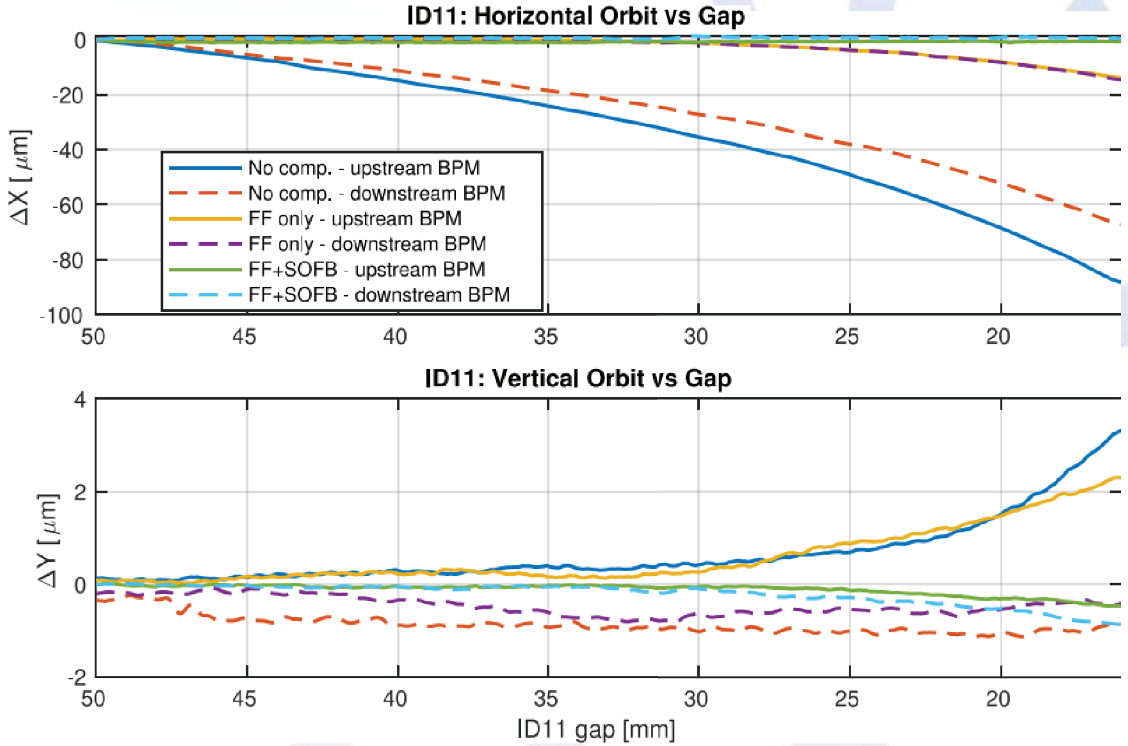

Horizontal and vertical orbit variation measured at the BPMs immediately upstream and downstream of the ID11 APPLE-II U56 undulator during gap changes. Three operating conditions are compared: no compensation, feed-forward only, and feedforward with SOFB enabled.

Towards FOFB

- The proposed FOFB architecture uses the existing Libera Brilliance+ BPM electronics and GDX modules to distribute fast orbit data from up to 48 BPMs around the storage ring.
- The GDX modules are interconnected through optical fiber links in a daisy-chain configuration, forming the Libera Grouping network and distributing the FA position data among the participating chassis.
- The global orbit data are provided simultaneously to the FA Archiver for high-rate beam-motion analysis and to a dedicated CPU-based calculation node, where the orbit correction is computed.
- The resulting horizontal and vertical correction setpoints are transmitted through separate power-supply gateways and controllers to the 64 corrector magnets, 32 in each plane. This architecture is designed as a single global feedback loop acting simultaneously in both transverse planes while making maximum use of the existing SESAME hardware.

10 / 12
GDX modules installed

40 / 48
fast BPMs now reachable

10 kS/s
server processing demonstrated

≈5 kS/s
gateway maximum

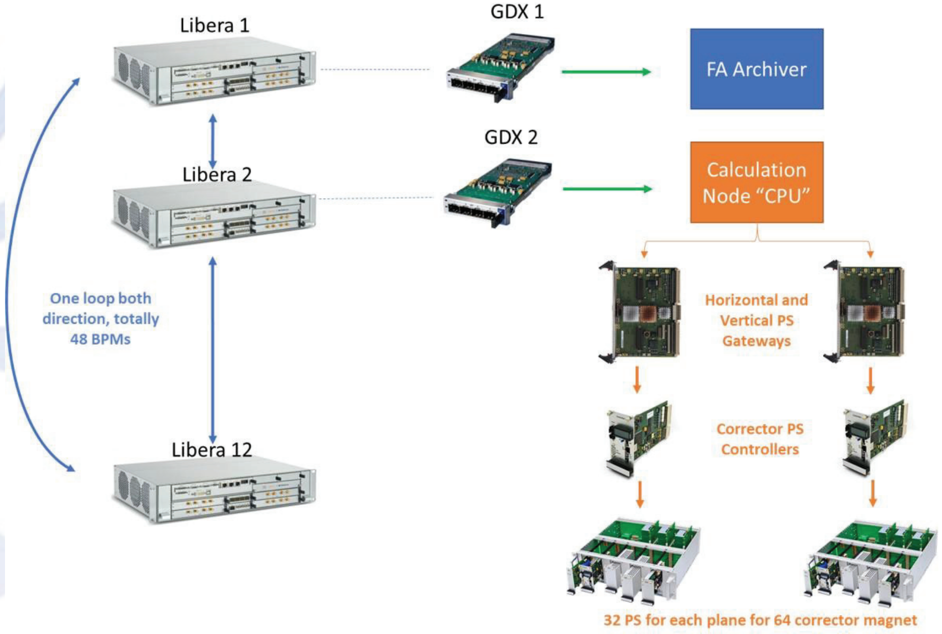

Towards FOFB

- A dedicated Fast Acquisition (FA) archiver has been implemented The system is based on the FA Archiver developed at Diamond Light Source
- Synchronized BPM position data are continuously recorded at the 10 kHz FA rate for orbit analysis and feedback studies. The archiver records the available horizontal and vertical BPM FA data into a rolling buffer with a storage capacity of approximately 12 days.
- This provides a continuously available fast orbit history and effectively acts as a large post-mortem buffer for investigating orbit disturbances after they occur.

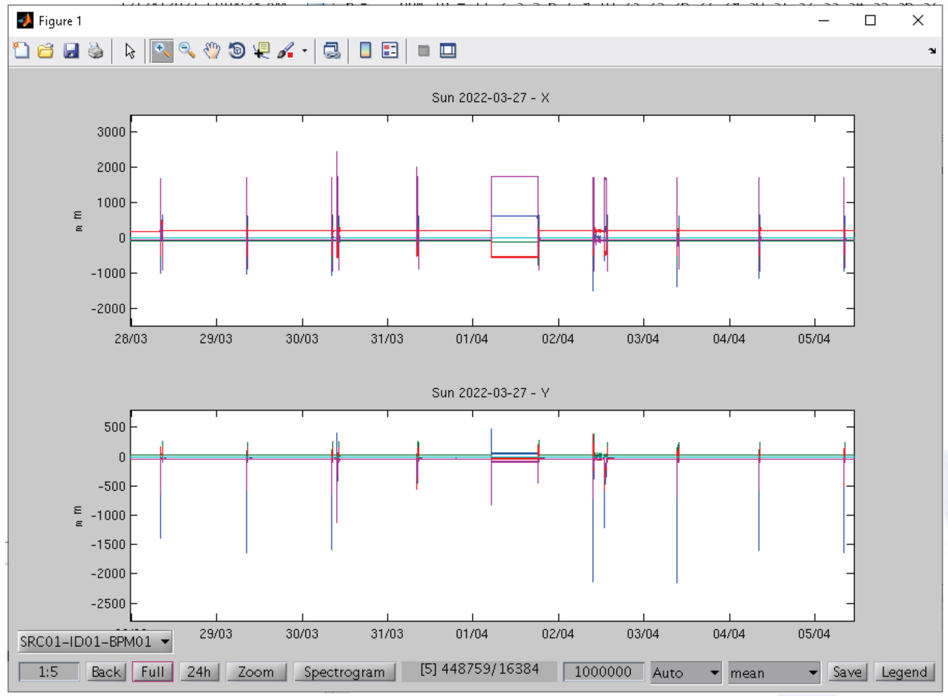

FA Archiver GUI

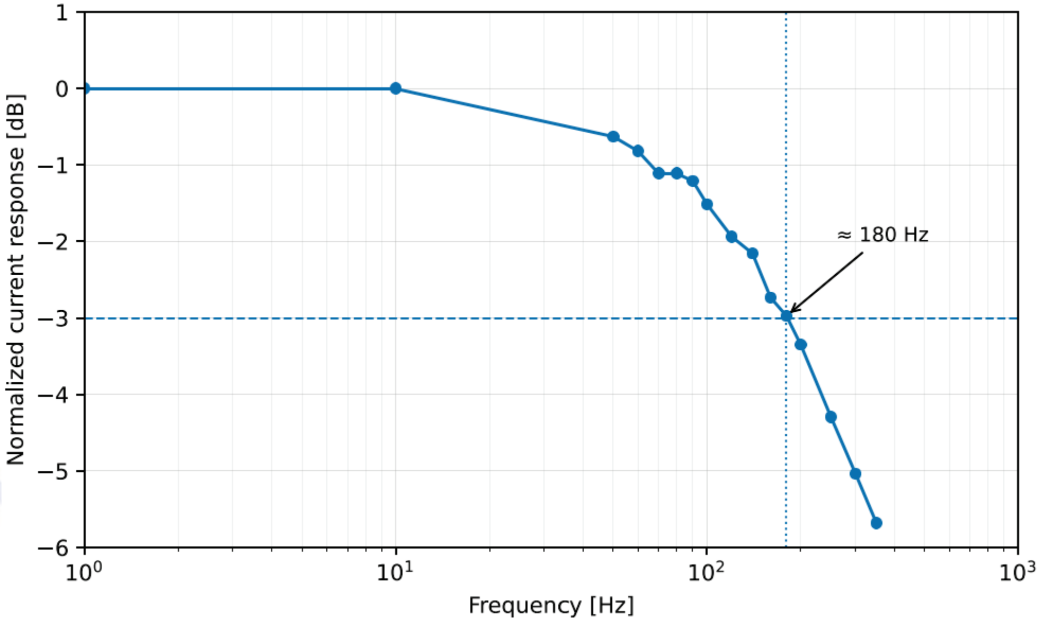

The frequency response of the corrector power supply was measured using a 100 mA peak-to-peak sinusoidal reference, showing an electrical −3 dB bandwidth of approximately 180 Hz.

Is Beam Position Stable ? YES!

SESAME

- The current orbit stability (<10% of beam size) does not require a FOFB system.

RMS in 1-100Hz		Horizontal			Vertical		
		Long Straight	Short Straight	Dipole	Long Straight	Short Straight	Dipole
Position (μm)	Limit	82.59 (10%)	82.08 (10%)	23.23 (10%)	2.08 (10%)	1.42 (10%)	8.1 (10%)
	SOFB+FF (Current)	8.94 (1.08%)	9.4 (1.145%)	5.6(2.41%)	1.4 (6.73%)	0.46 (3.24%)	1.99(2.5%)

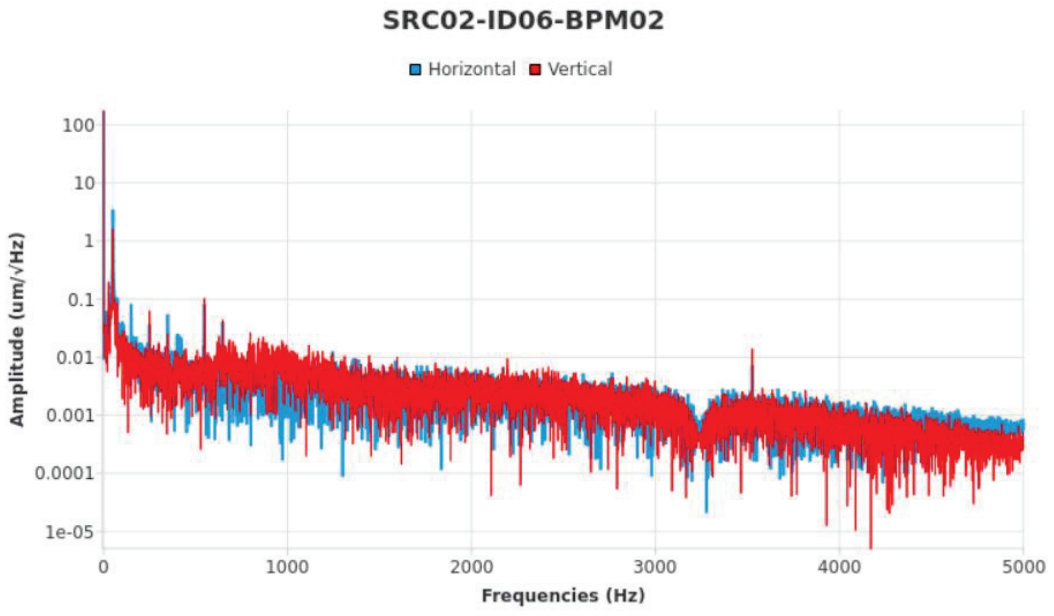

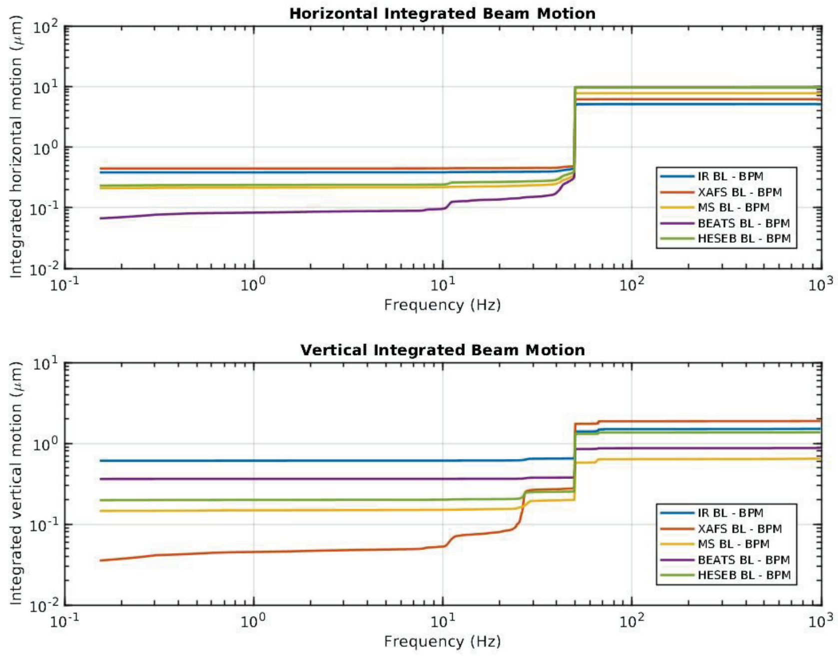

FOFB

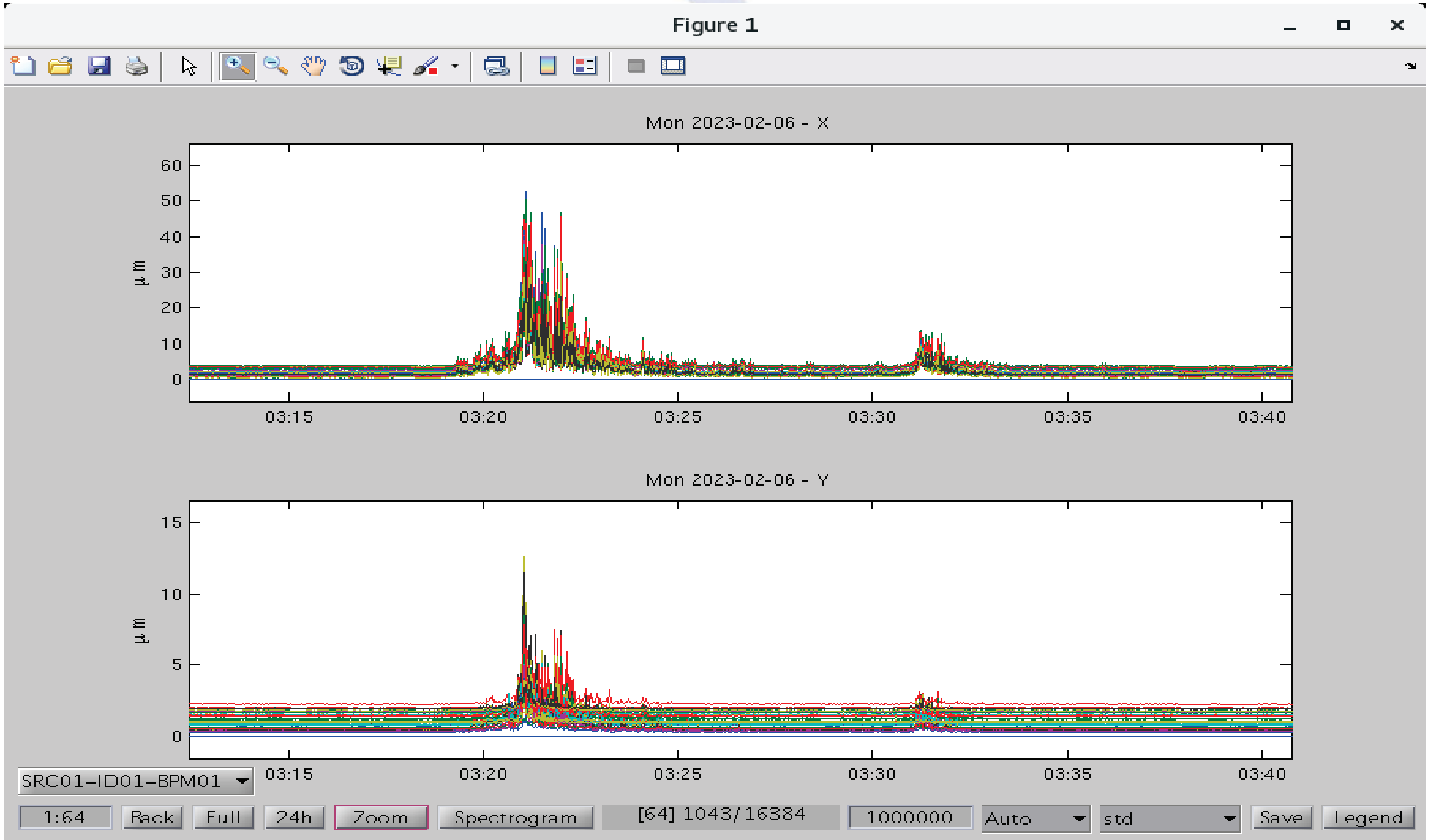

Turkish earthquake 2023 detected by our SR BPMs and orbit feedback return the orbit to its original position.

Beam Size Measurement

Beam Size Measurement

- Pinhole camera : A simple, robust and power horse tool to measure beam size.
- Original design to have an aluminum window with copper absorber to let part of X-rays goes to pinhole assembly.
- Due to limited budget the project postpone for a while.
- There was visible beamline inside the SR tunnel , an incident happened to its view port and damage the copper mirror.
- While investigating the mirror an idea comes why not to reuse it as absorber for pinhole and have a copper window instead of aluminum one !
- Simulation and calculations were done on Ansys, XOP, SHADOW to ensure working principle and can handle the x-rays with thin layer of copper.

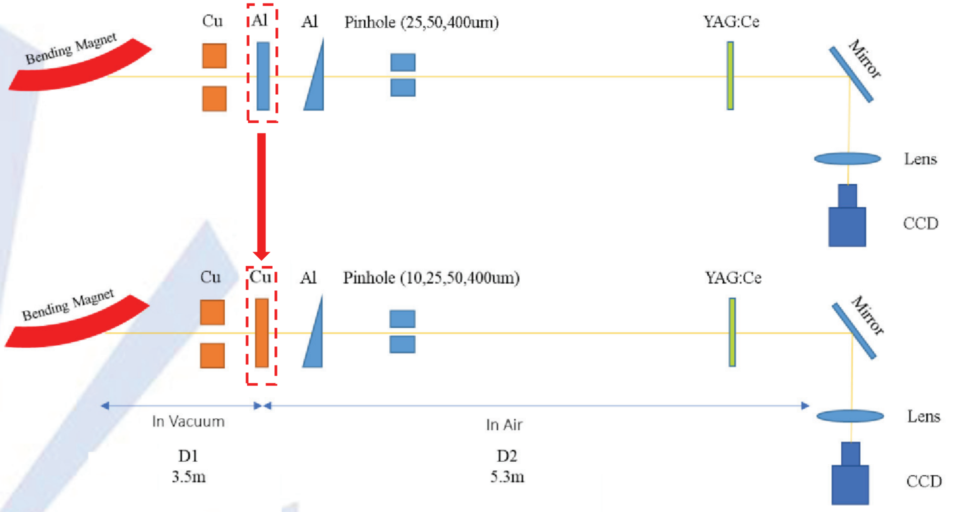

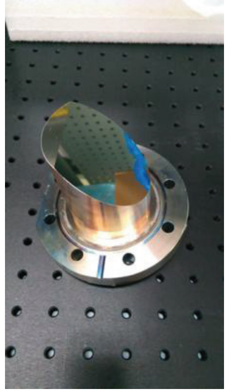
Before incident

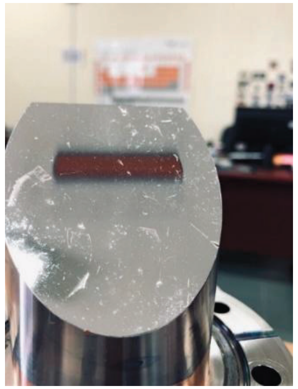
After incident

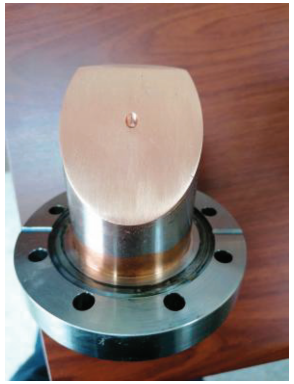
After modification

Modified absorber

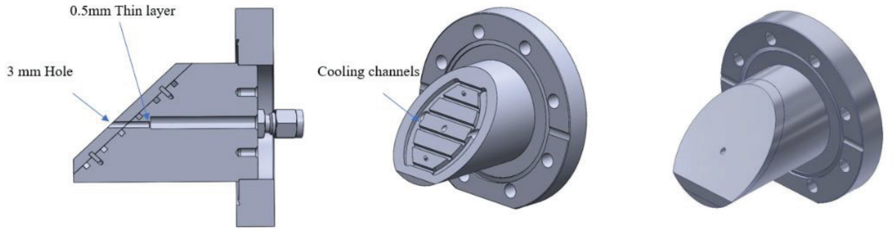

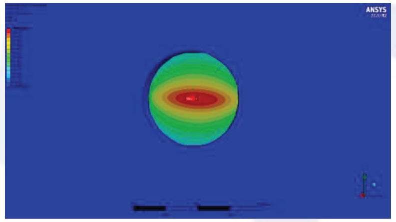

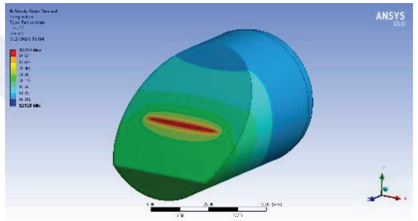

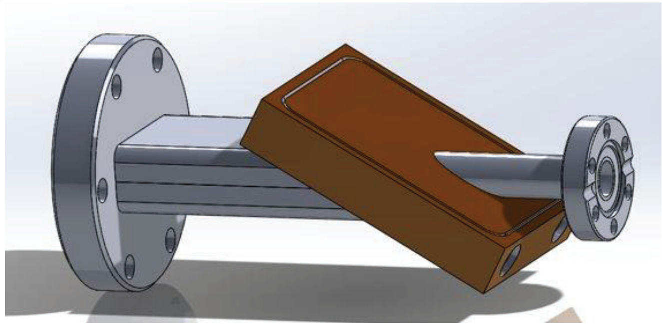
Original absorber design

Pinhole

- 5 degree of freedom motorized stage used for pinhole assembly movement, YAG:Ce Scintillator, 400,50,25,15 um pinholes using tungsten blades separated by shims

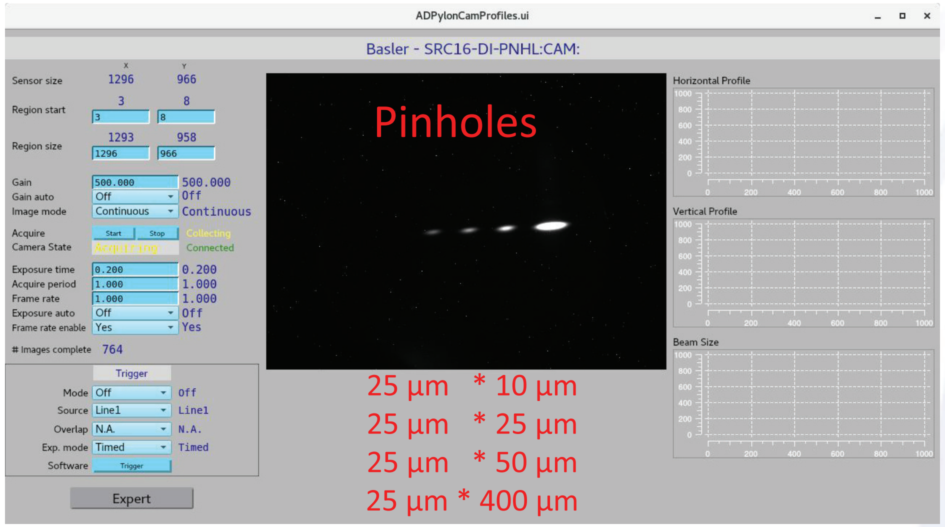

Absorber

YAG screen

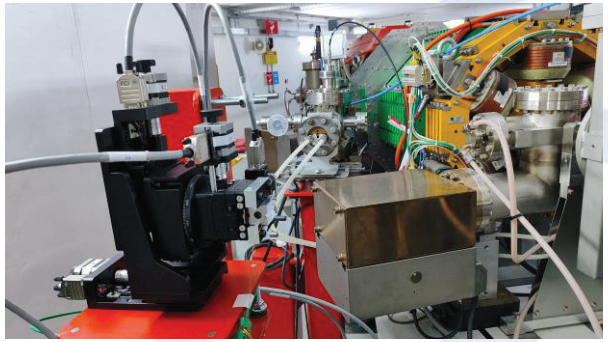

motorized stage and pinhole assembly

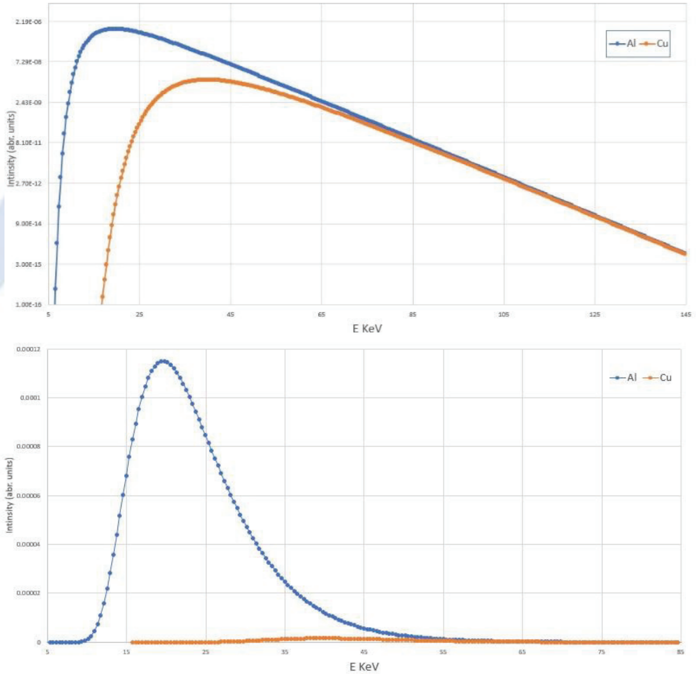

Spectrum of extracted X-ray photon beam showing how copper attenuate the intensity and shift the energy in logarithmic scale (up) linear (down).

H. Al-Mohammad, A. Hasoneh, M. A. Shehab, and O. Kailani, “An X-Ray Pinhole Camera for SESAME Storage Ring”, in Proc. IBIC’24, doi:10.18429/JACoW-IBIC2024-WEP04

Pinhole

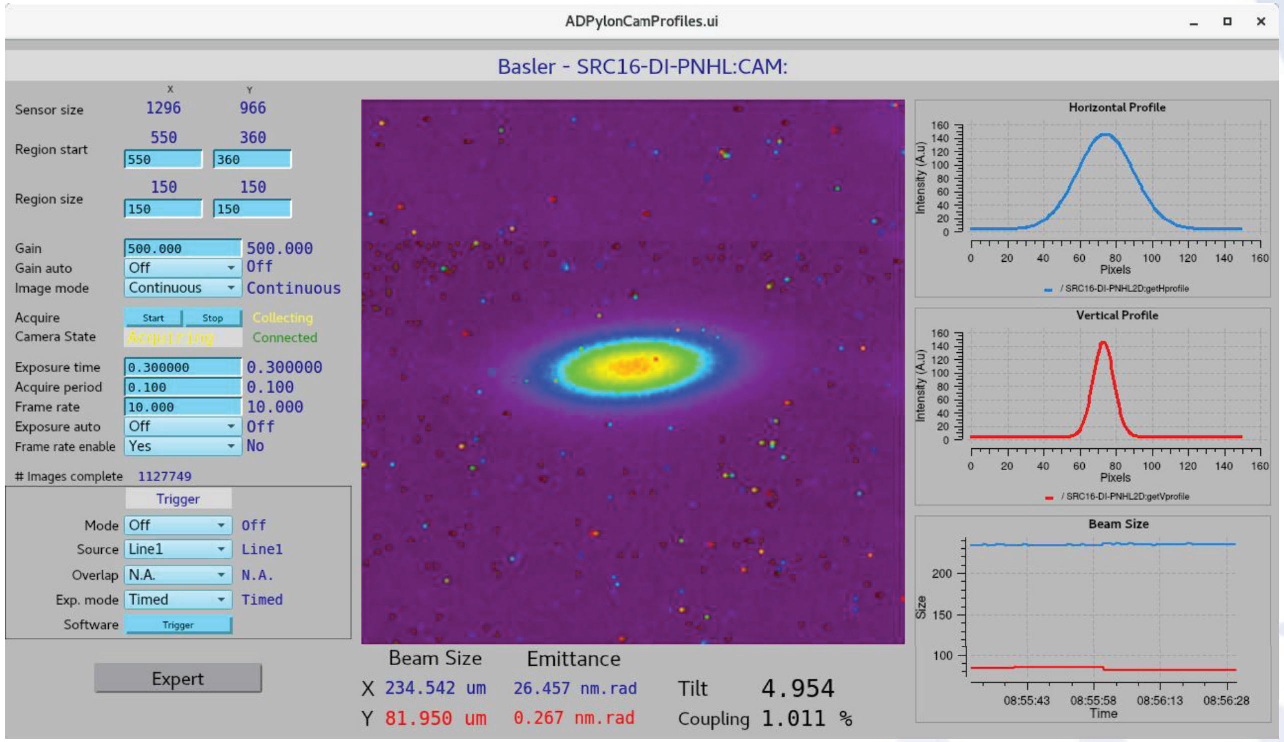

	Designed	Measured
σx	232 µm	231 µm
σy	81 µm	81.9 µm
εx nm.rad	26	26.457
εy nm.rad	0.26	0.267
Coupling %	1	1.011

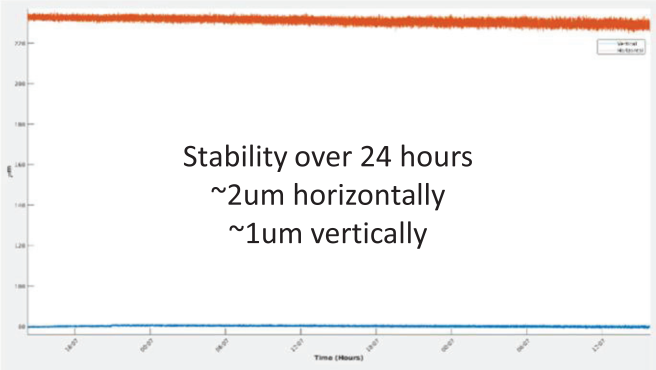

Visible Diagnostics Beamline-VDBL

- An idea is coming up to solve the issues of the visible beamline inside the tunnel especially alignment and focusing of cameras.
- Guide the light to outside the tunnel will allow to do experiments to measure the beam size beside other future development like bunch length and stability measurements.
- Beam size measurement using double slit interferometer in both plane were performed.
- The design kept as simple as possible and with the minimum cost by using all available components.

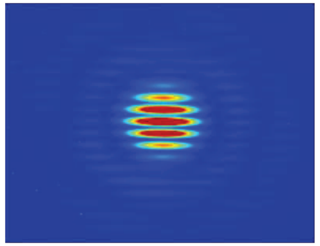

$$V = \frac{I_{max} - I_{min}}{I_{max} + I_{min}}$$

$$\sigma = \frac{\lambda L}{\pi D}\sqrt{0.5 \ln\left(\frac{1}{V}\right)}$$

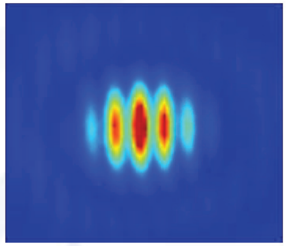

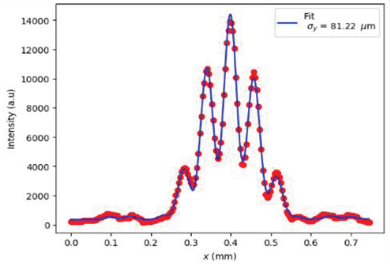

	Interferometry	Pinhole
σx	231.2 μm	231 μm
σy	81.22 μm	80.82 μm

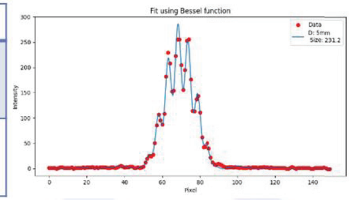

Vertical interferogram with fitting using 4mm slit separation.

Horizontal interferogram image with fitting using 5mm slit separation

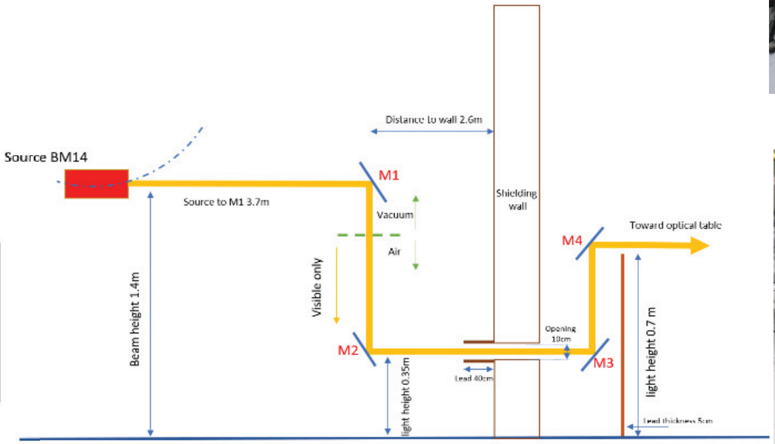

Schematic layout for visible diagnostics beamline from inside to outside tunnel.

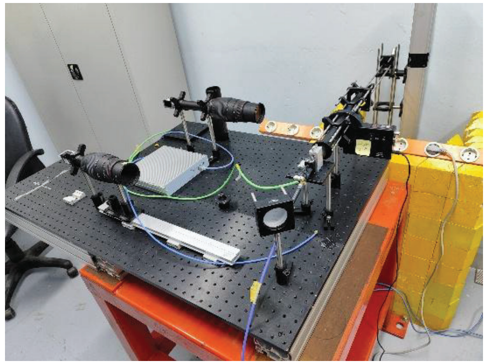

Optical table inside hutch

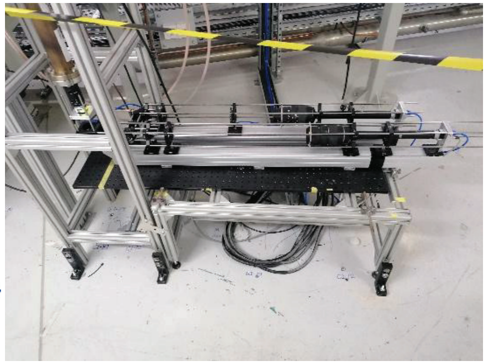

Old setup inside tunnel

H. Al-Mohammad, A. Hasoneh, M.Al-Najdawi, “Diagnostics Visible Beamline At Sesame Storage Ring ”, inProc. IBIC’24, doi: 10.18429/JACoW-IBIC2024-WEP05

In Air X-Ray Detector- IAXD

MOP049

- X-ray pinhole cameras provide reliable beam size measurements, but they are normally available only at dedicated source points. Additional compact diagnostics tool distributed around the SR can therefore provide complementary information on the local beam parameters.

- The IAXD uses the **unused hard X-rays from a bending magnet that penetrate the photon absorber**. These X-rays are converted into visible light by a scintillator and imaged with a camera. The measured vertical X-ray profile contains contributions from the **electron beam size and divergence, together with the photon divergence**. Using the known **source-to-screen distance** and photon divergence, these contributions are deconvolved to determine the **vertical electron beam size at the dipole source point**.

$$\sigma_{ph} = \sqrt{\sigma_y^2 + L^2\left(\alpha_{ph}^2 + \alpha_e^2\right)},$$

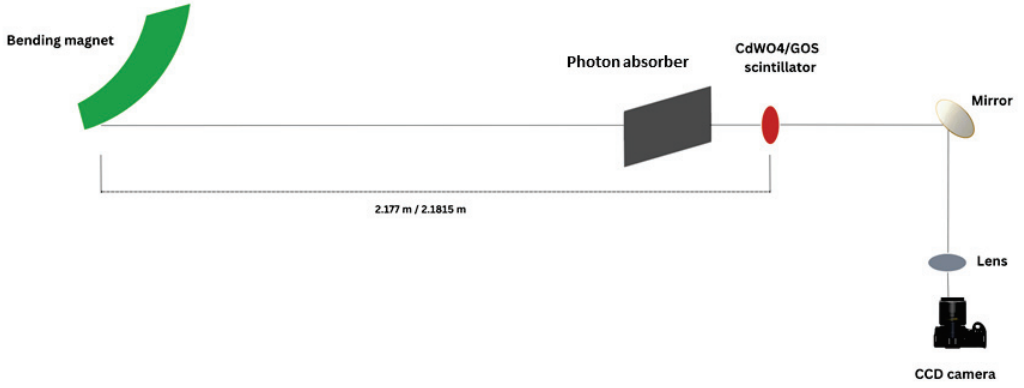

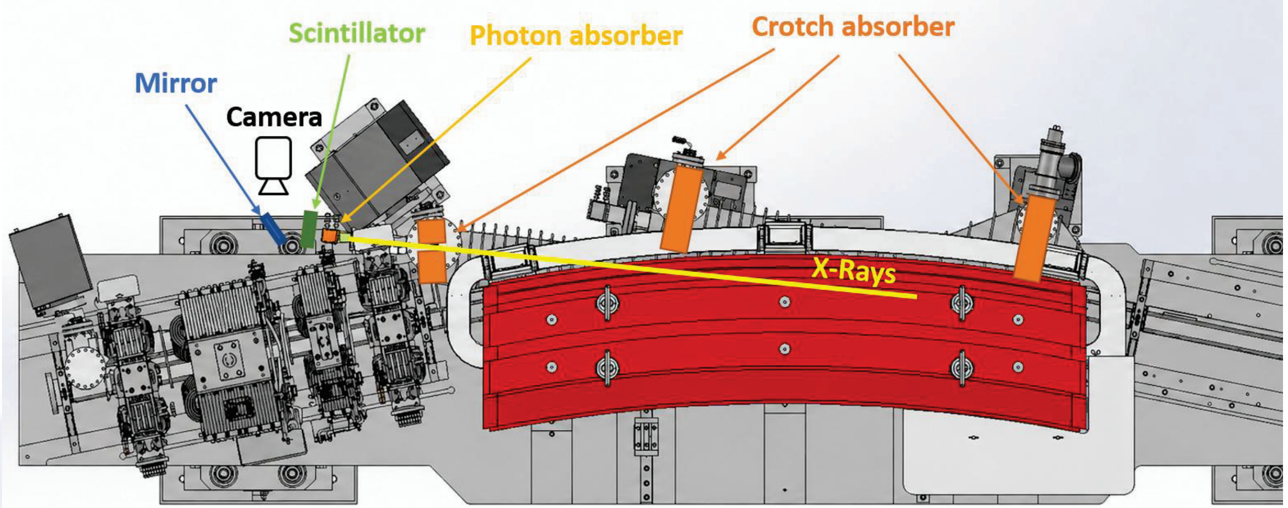

In Air X-Ray Detector- IAXD

- IAXD is used in multiple synchrotrons facilities (designed by ESRF , applied at KARA, ALBA and SOLEIL) installed it after **crotch absorber**.

- At **SESAME**, the crotch absorber is ~30mm thick followed by 3mm stainless steel vacuum chamber, initial transmission calculations showed that the combined attenuation through the crotch absorber and chamber wall reduces the remaining hard X-ray intensity to a level too low for practical imaging.
- A photon absorber located at 6.5° BM port not used by a beamline is chosen where the effective copper thickness is less and sufficient hard X-ray intensity is transmitted so it can pass the hard X-rays from selected source point corresponds to the photon path through the absorber cooling-channel region.

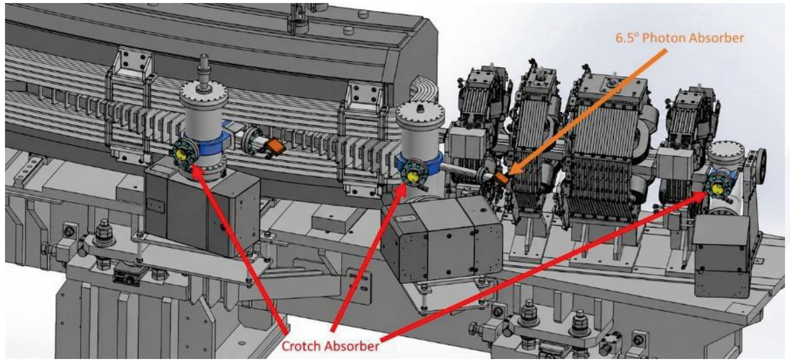

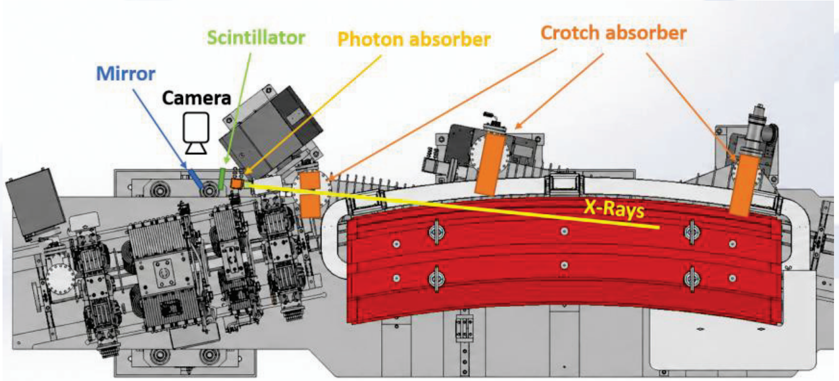

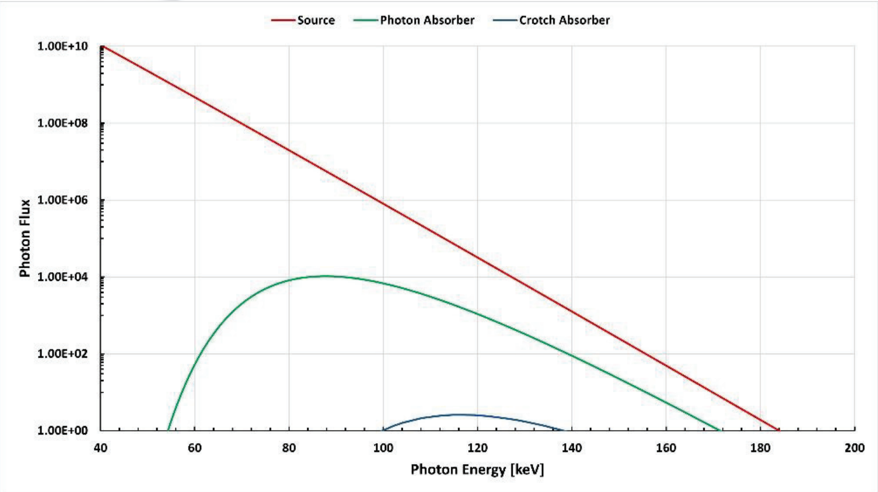

IAXD

- The photon path crosses the absorber at about **30°** inclined copper, giving an effective copper thickness of roughly **30 mm**, while the internal cooling channel locally reduces the thickness to about **11 mm**.
- This reduced-thickness region provides a localized high-transmission path for the hard X-rays and defines the useful footprint observed by the IAXD.
- The synchrotron-radiation spectrum and transmission were calculated with **XOP**, including the source spectrum, copper attenuation, and scintillator absorption. After the absorber and screen, the useful spectrum is concentrated around ~**87 keV**.
- **SHADOW/OASYS ray tracing** was then used to evaluate the photon-beam geometry at the detector and relate the measured vertical photon profile to the expected electron beam size at the selected source point.
- 0.5mm $CdWO_4$ scintillator used as the 1^{st} prototype.

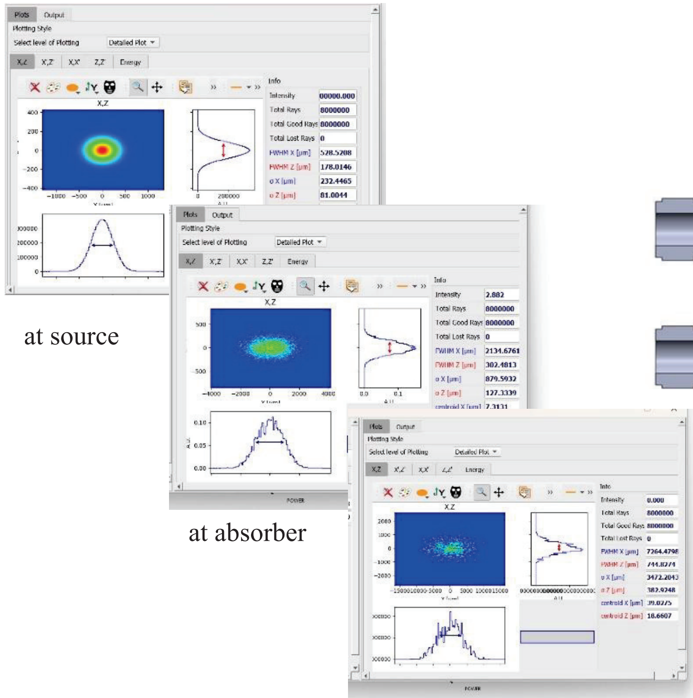

at source

at absorber

at scintillator

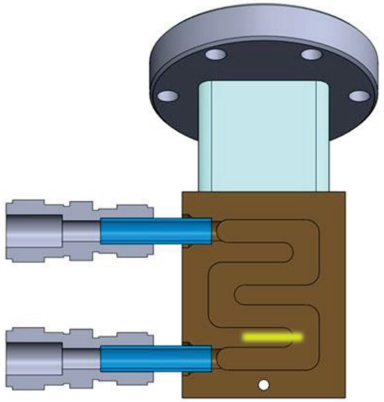

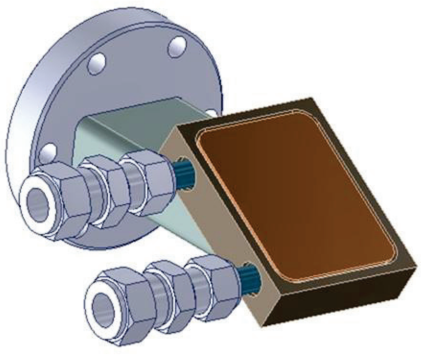

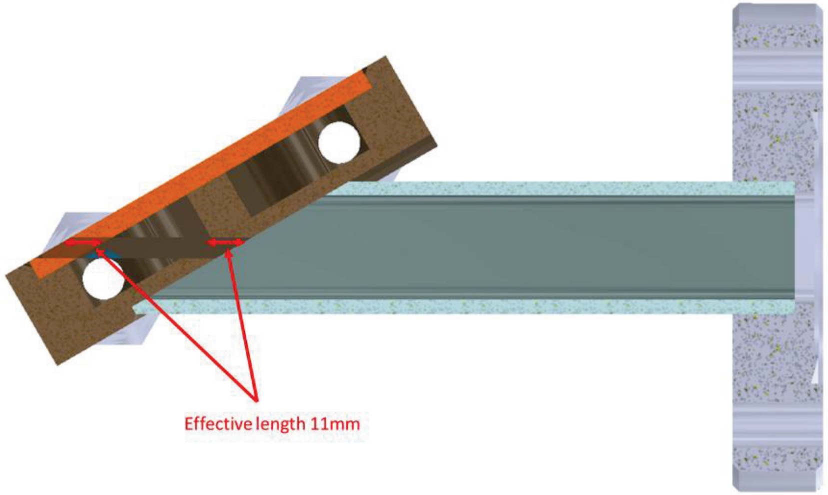

SESAME

IAXD

- Two scintillators were evaluated: **CdWO4** and **GOS:Tb**. CdWO4 was selected initially because it is a dense, high-Z crystal already demonstrated for in-air hard X-ray diagnostics at other synchrotrons.
- **GOS:Tb provides a substantially higher light yield** than CdWO4, so it gives a brighter visible signal for the same transmitted hard-X-ray beam and allows shorter camera exposure times.
- At SESAME, the transmitted spectrum after the copper absorber is concentrated around ~**87 keV at 6.85° angle** ; the scintillator absorption was included in the intensity calculation to estimate the useful detected photon signal.
- Experimentally, the GOS:Tb screen produced comparable beam images with a **significantly shorter exposure time** (3.5s) than CdWO4(8s), making it more suitable for routine beam-size monitoring.
- The detector is a compact in-air system consisting of a **scintillator screen, mirror, imaging optics, and camera**.

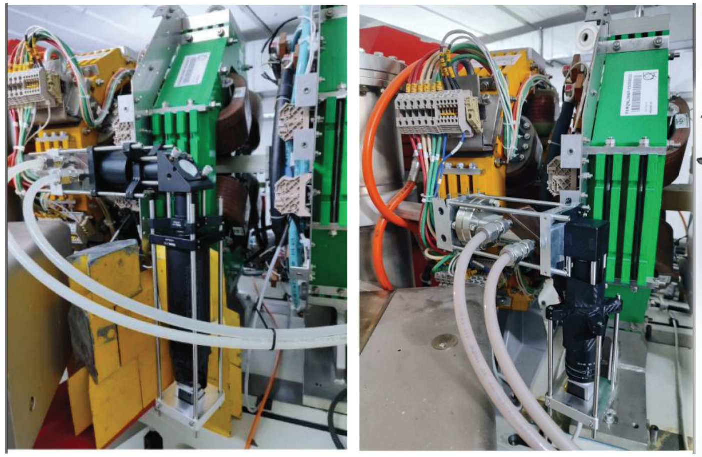

Two detectors installed in cell 6 and 3

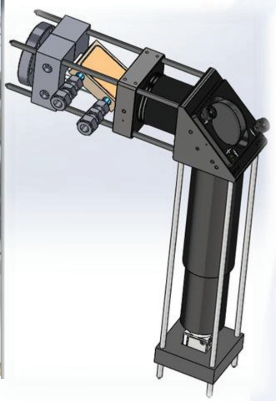

The 1st version hold CdWO4 with 2 inch optical system

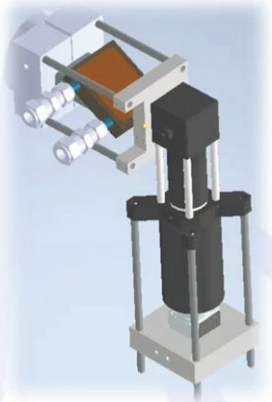

The 2nd version hold GOS with 1 inch optical system

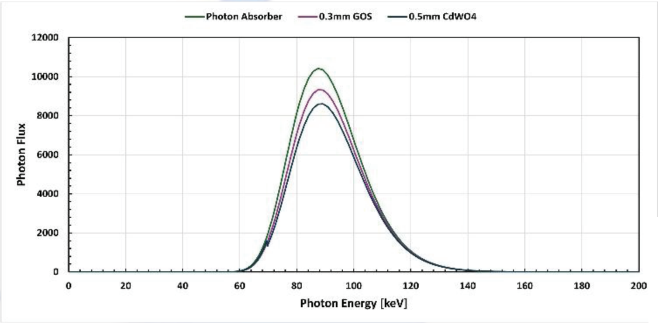

XOP-calculated photon spectrum downstream the photon absorber and after transmission through the 0.5 mm CdWO4 and 0.3 mm GOS scintillation screens.

Table 1: Properties of the IAXD Scintillation Screens

Property	$CdWO_4$	GOS:Tb
Thickness (mm)	0.5	0.3
Density (g/cm^3)	7.9	7.34
Emission peak (nm)	475	550
Light yield (photons/MeV)	12000-15000	46500
Screen form	Crystal	Ceramic

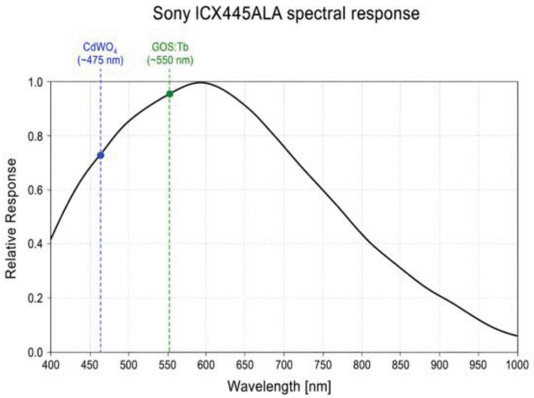

IAXD

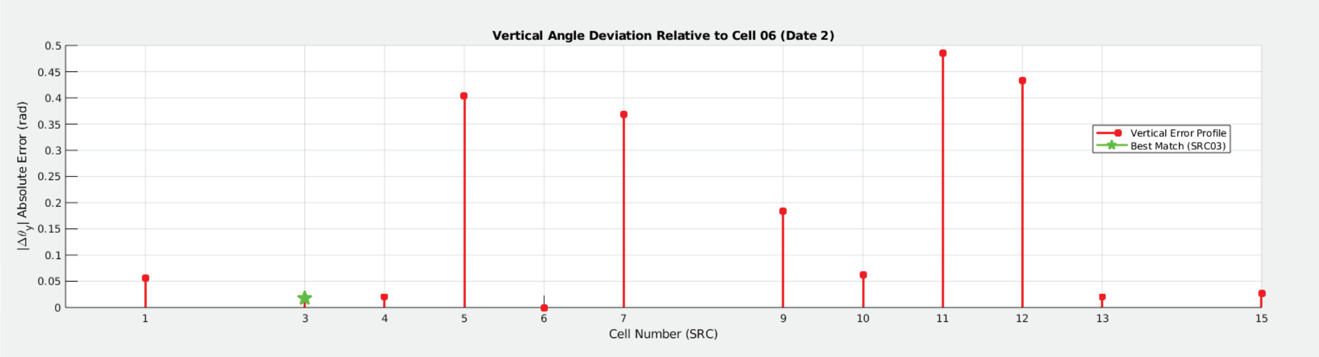

Calculation to find best match cell to cell 6 where the prototype is installed and match good beam angle to see higher intensity

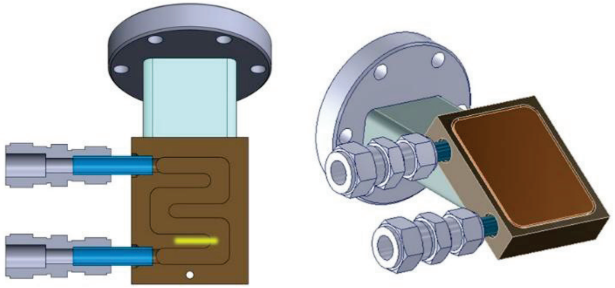

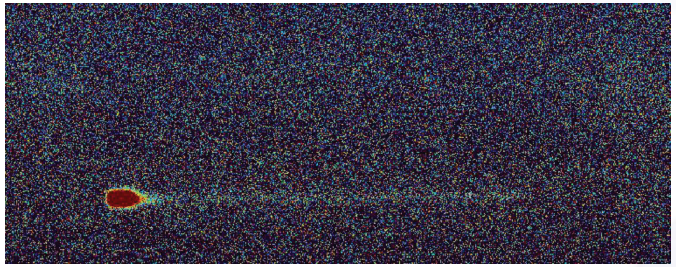

First beam observed with the IAXD (10 s exposure time), showing the beam spot and the faint horizontal line produced by radiation transmitted through the adjacent copper region.

Beam spots obtained with CdWO4 (top left) and GOS:Tb (top right), with the corresponding vertical profiles shown below.
CdWO4 use 8 seconds exposure time while GOS use ~3.5 seconds

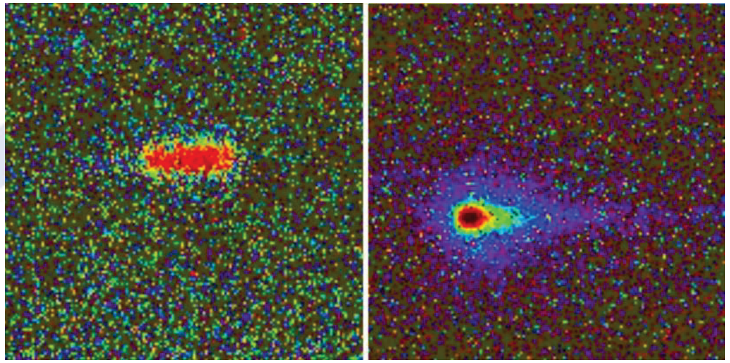

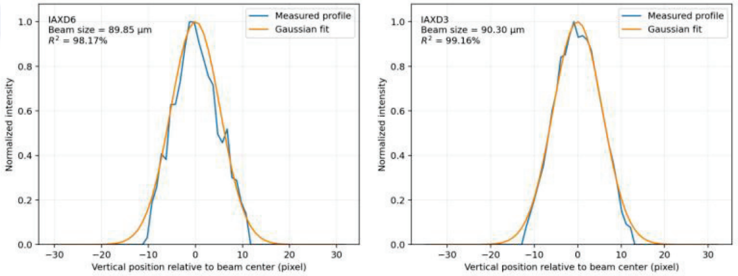

IAXD

- The IAXD images are processed through a compact sequence developed to isolate the beam footprint and provide a robust beam-size measurement. A dynamic intensity threshold is first applied to separate the beam signal from the background, followed by morphological erosion and dilation to suppress isolated noise and improve the continuity of the detected region.

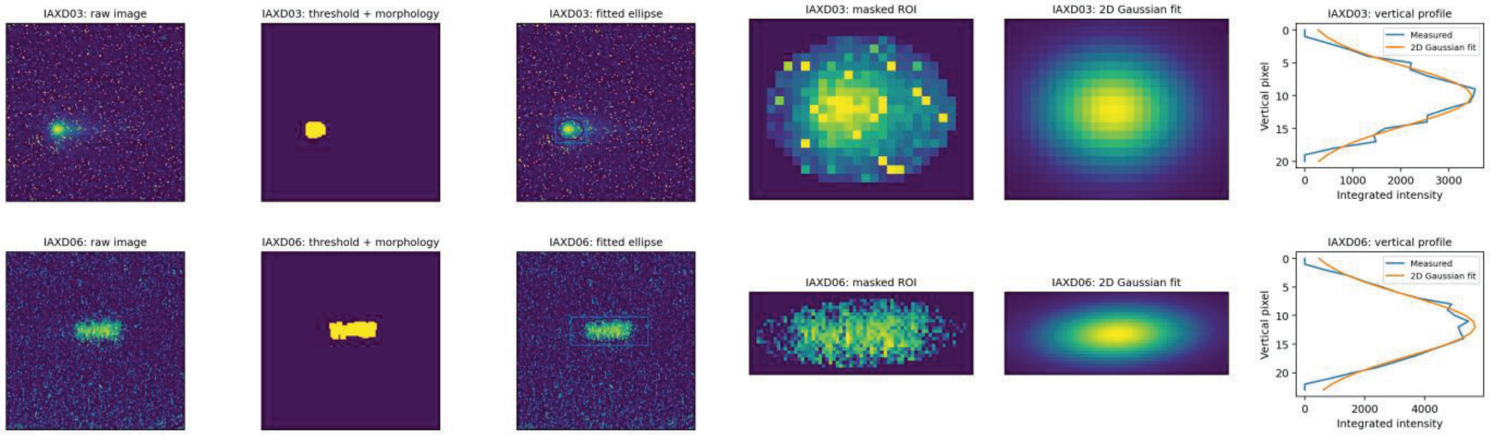

Raw image → Dynamic threshold → Erosion + dilation → Largest component → Ellipse mask → ROI crop → 2D Gaussian fit → Vertical profile

88.7 µm
model calculation

≈90 µm
measured by IAXDs

Result: the measured beam sizes agree with the model and expected size at the IAXD locations.

The stronger GOS signal and compact Cell 3 configuration improved practical profile measurement.

IAXD

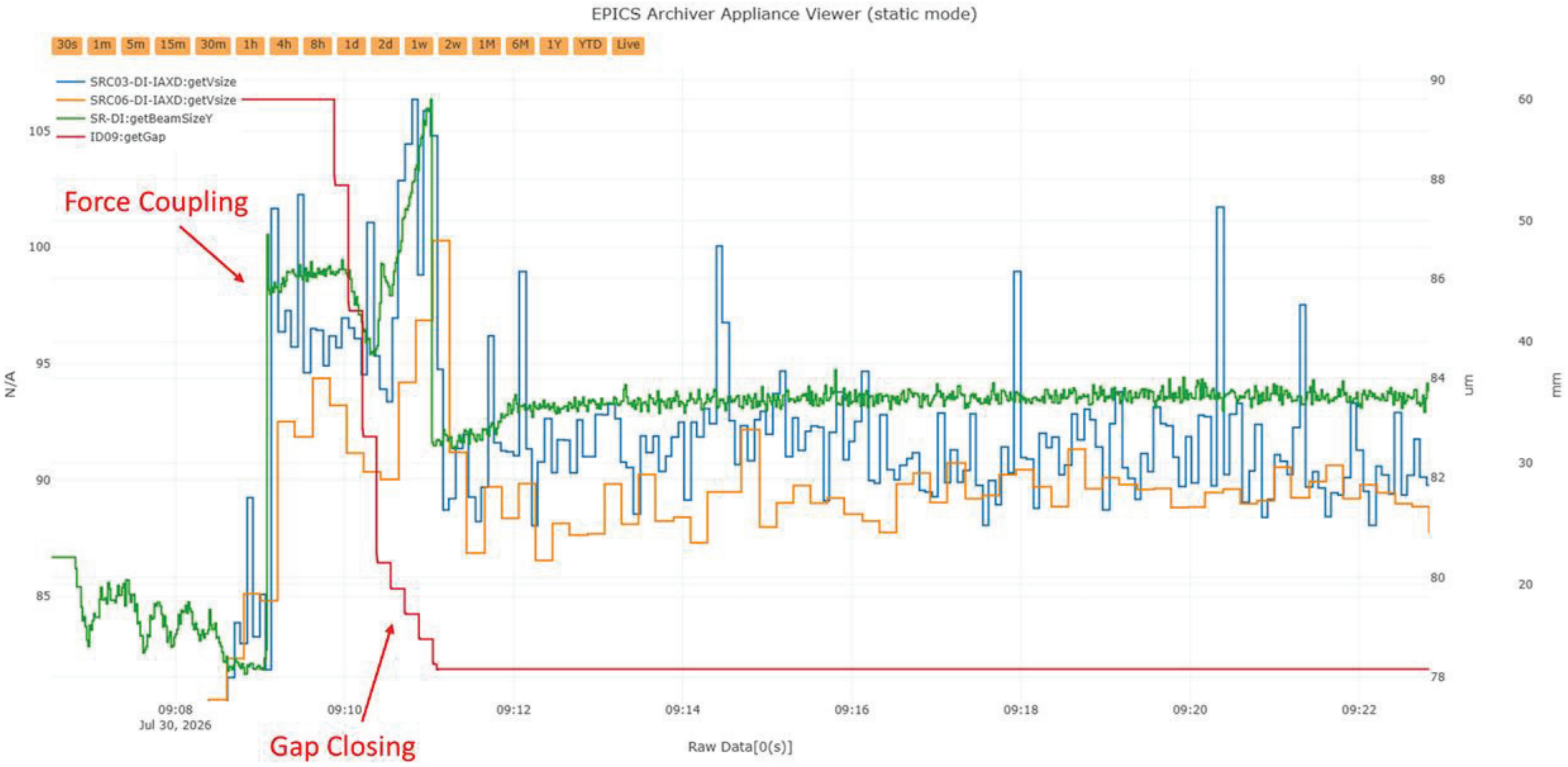

Vertical beam size measured by IAXD03, IAXD06, and the X-ray pinhole camera during user operation, showing the response to forced coupling and ID09 gap closure.

Injection Efficiency Measurement

Injection Efficiency

SESAME

TUP044

Injection efficiency is an important indicator of accelerator performance, reflecting how effectively the electron beam is transported from the booster to the storage ring. Reliable monitoring helps identify losses during extraction, transmission , and injection, supports machine optimization, and is particularly important for stable and efficient user operation. Combine current transformers, DCCTs, FTCs and BPM-based measurements to evaluate beam transmission at different stages of the injection chain.

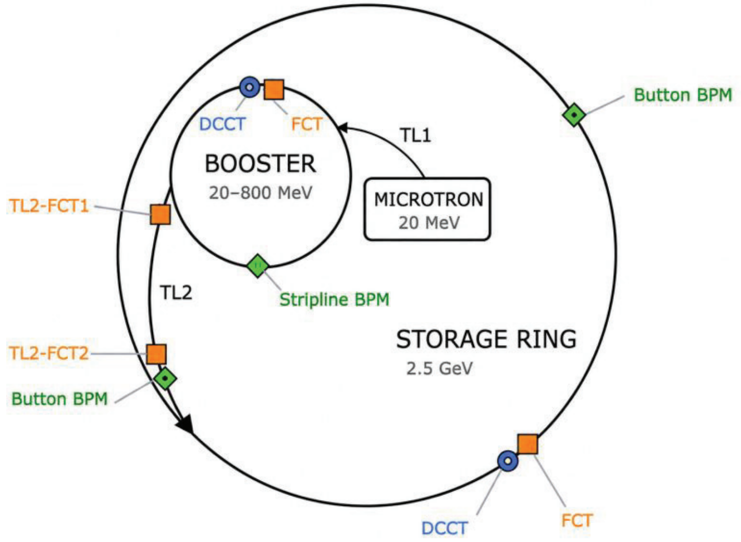

DCCT + FCT + BPM
booster instruments

2 FCTs + BPM
TL2 transmission

DCCT + FCT + BPM
SR instruments

SESAME

Injection Efficiency

The injection efficiency is defined as the ratio of the charge accumulated in the storage ring to the charge extracted from the booster which = (extraction from BO) x (transmission through TL) x (injection to SR)

$$\eta_{\mathrm{tot}} = \frac{\Delta Q_{\mathrm{SR}}}{Q_{\mathrm{BO}}} \times 100\% = \eta_{\mathrm{ext}}\,\eta_{\mathrm{TL2}}\,\eta_{\mathrm{inj}}$$

DCCT-based

For the circulating beam, the measured current is converted to charge using the ring revolution frequency. The storage-ring injected charge is obtained from the current increase before and after injection.

$$Q_{\mathrm{DCCT}} = \frac{I_{\mathrm{DCCT}}}{f_{\mathrm{rev}}}$$

FCT-based

The beam charge is obtained by integrating the baseline-subtracted FCT waveform over the bunch-train window. This provides a direct single-pass charge measurement at different locations along the injection chain.

$$Q_{\mathrm{FCT}} = \frac{1}{Z_{\mathrm{t}}} \int_{t_1}^{t_2} [V(t) - V_0]\, \mathrm{d}t$$

BPM-based

The summed BPM electrode signal is used as a relative intensity measurement and calibrated against a nearby FCT to convert it into beam charge.

$$Q_{\mathrm{BPM},i} = C_i R_{\mathrm{BPM},i}$$

Injection Efficiency

DCCT-based

BO-DCCT

SR-DCCT

Keysight 34461a

FCT-based

BO- TL2 FCTs

SR-FCT

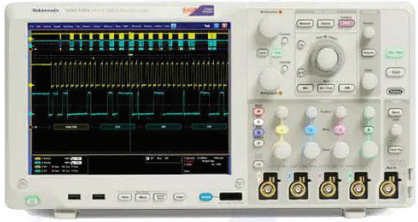

Tektronix DPO5104B
1GHz

Rigol MHO98
1GHz (12bit)

BPM-based

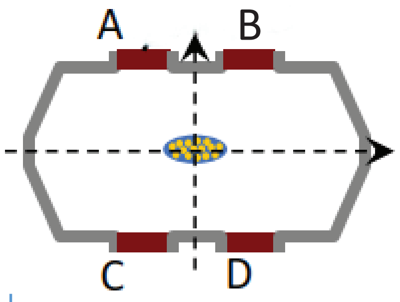

SR-BPM

BO,TL2 BPMs

Libera Brilliance+

Libera Electron

Synchronized triggers allow signals from different locations to be associated with the same injection event.

Injection Efficiency

Electromagnetic interference from the extraction and injection pulsed elements affected the current-transformer signals. Additional shielding and bonding around the kickers, septums, and SR current transformers reduced the pickup by about a factor of two. Residual interference on TL2-FCT1 was corrected by subtracting a kicker-only reference waveform acquired without beam.

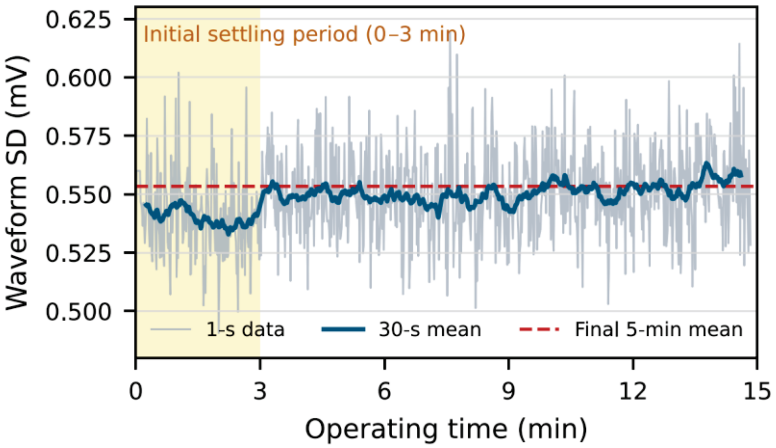

TL2-FCT1 reference waveform SD stability over 15 min, showing an initial ~3 min settling period followed by stable operation around 0.55 mV.

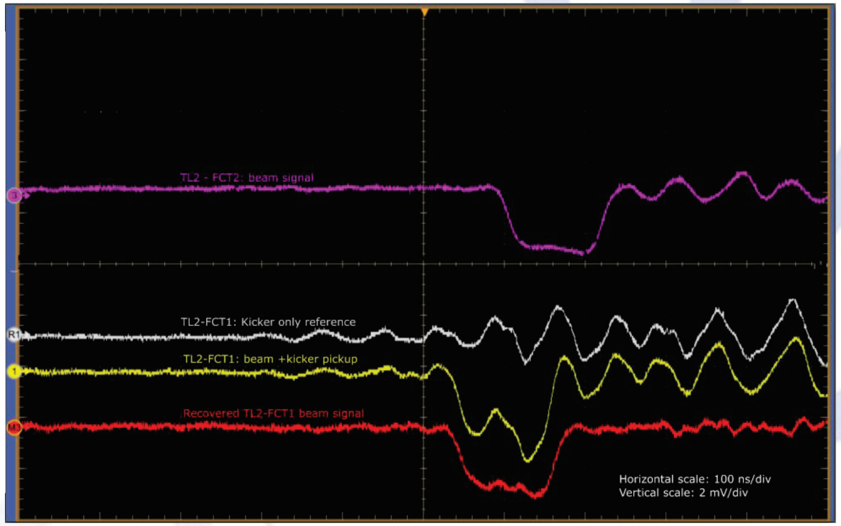

TL2-FCT1 signal affected by extraction kicker pickup (yellow) and the recovered beam signal after subtraction (red) of a kicker-only reference waveform (white). The TL2-FCT2 beam signal is shown for comparison.

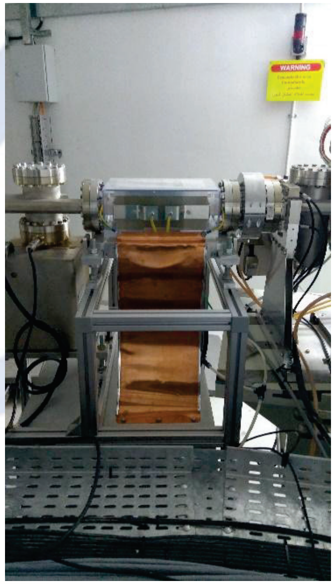

Copper sheets installed on one of pulse elements and another one to DCCT+FCT shield

SESAME

Injection Efficiency

The three measurement methods showed consistent overall injection-efficiency trends. The **DCCT-based method** gave the most stable result, with a mean total efficiency of about **36.3%**. The **FCT-based method** gave about **31.0%**, with some remaining uncertainty from kicker-background subtraction and charge calibration. The **BPM-based method** yielded about **33.6%** and showed larger cycle-to-cycle variations. The BPM measurements also indicated a mean combined **booster extraction + TL2 transmission efficiency of 69.7%**, while the largest fluctuations were observed during injection into the storage ring. Overall, the agreement of the three independent methods validates the measurement approach and helps identify where the main beam losses occur.

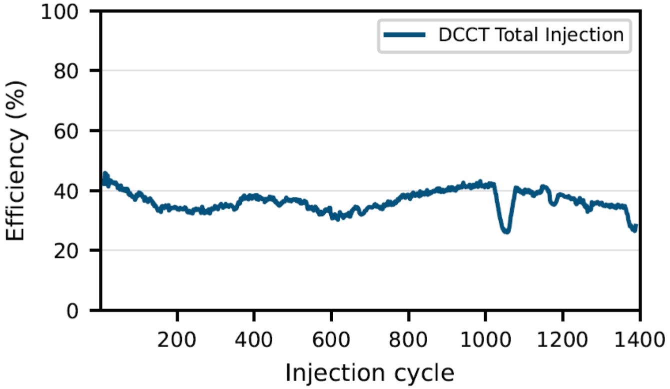

DCCT-based total injection efficiency.

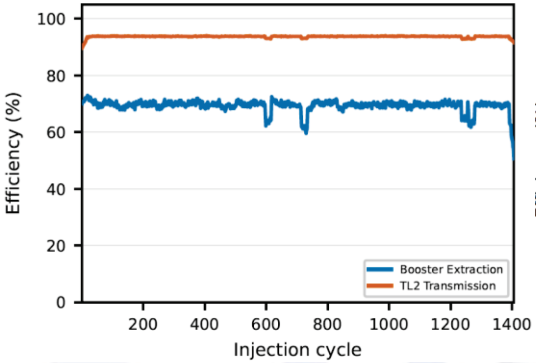

FCT-based BO Extraction and TL2 Transmission Efficiencies.

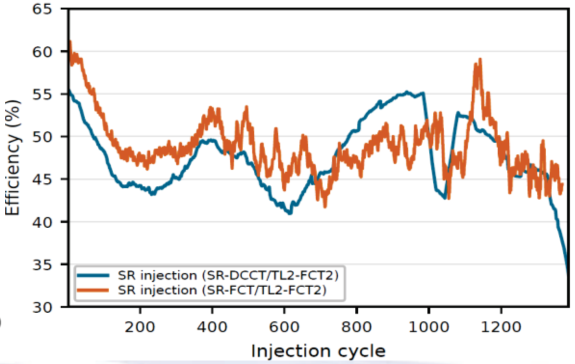

SR injection efficiencies obtained from SRDCCT/TL2-FCT2 and SR-FCT/TL2-FCT2.

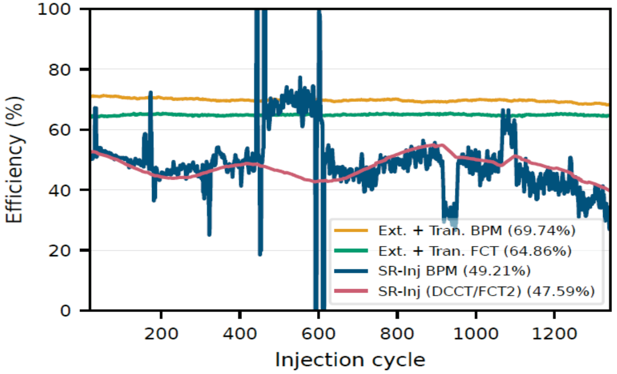

Comparison of BPM and FCT/DCCT injection efficiency measurements over successive injection cycles.

Injection Efficiency

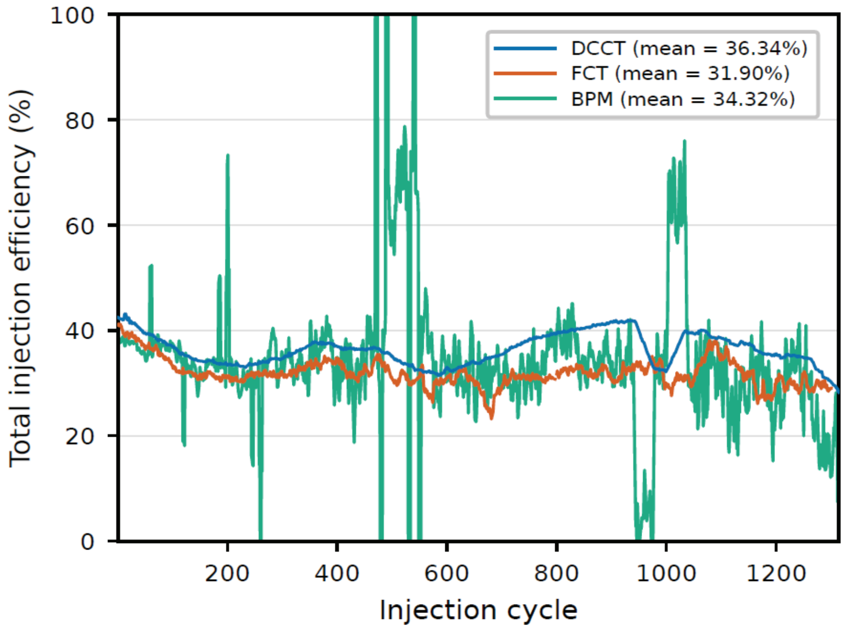

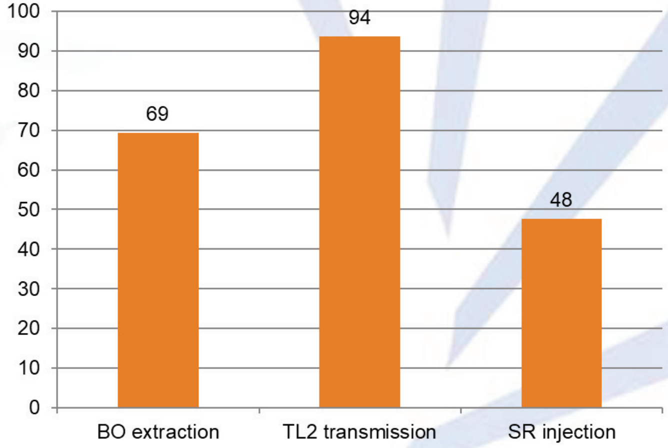

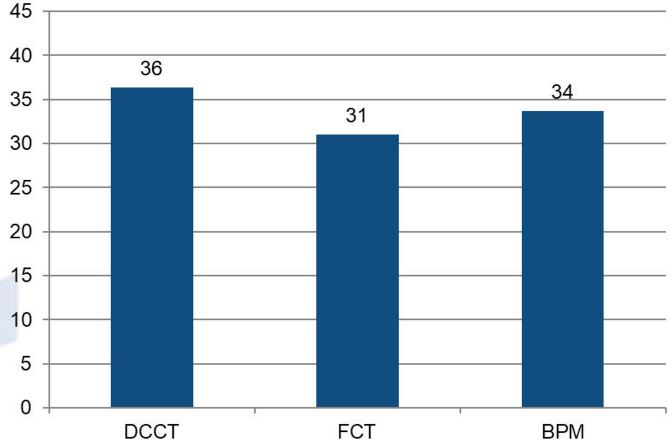

Comparison of the total injection efficiencies

Conclusions

SESAME continues to improve its beam diagnostics to support reliable operation and higher beam stability.

- The **orbit feedback system** provides stable beam operation, while the ongoing FOFB development is extending the system toward faster orbit correction and be ready for full energy booster.
- The **IAXD** provides a practical non-invasive method for monitoring the vertical electron beam size using available synchrotron radiation from an unoccupied dipole beamline.
- The **injection-efficiency measurements**, using DCCTs, FCTs, and BPMs, provide complementary information for evaluating the overall injection performance and identifying losses along the injection chain.

Together, these developments strengthen SESAME's diagnostic capabilities and provide the basis for future machine-performance improvements.


Thank You!